Contactless Person Identification Based on Double-sided 3D Scan of Hand Geometry

Piotr Stefan Nowak, Wojciech Sankowski, Paweł Krotewicz, and Mariusz Zubert

***Abstract*—This paper presents person identification algorithm based on 3D hand geometry. The algorithm comprises the following phases of 3D hand scan processing: segmentation, feature extraction and comparison, which the authors explain in detail in the paper. The authors present results of algorithm performance tested on publicly available *DMCSv1* database which contains 1400 samples of 3D hand scans of left and right hand acquired from 35 individuals. Obtained values of equal error rate are 16% for the left hand scans, 17% for the right hand scans and the values of rank-1 accuracy are 85% and 82% for the left and right hand scans, respectively.**

***Index Terms*—biometrics, contactless identification, hand recognition**

I. Introduction

We live in the world where importance of reliable, comfortable and fast person identification systems is increasing. Reliability can be achieved by means of multimodal biometric recognition [1] and introduction of novel traits. In first hand identification systems user was obliged to place his hand on a flat surface. A lot of currently working identification systems still require user to touch a device. This approach can be regarded unhygienic. With higher availability of 3D scanning systems recently researchers attempt to develop methods for 3D contactless person identification. According to the authors' knowledge modern scanning systems designed for development of algorithms for person identification described in the literature use single 3D scanning head [2]. The algorithms developed based on those systems calculate hand geometry features taking into account one side of a hand.

Algorithm presented in this paper is dedicated for Multimodal Biometric System for Contactless Person Identification (MBS) [3]. The system contains 3D data acquisition station presented in Fig. 1 and was used to acquire the *DMCSv1* database [4] which is publicly available to research and educational institutions. The database contains 3D face and hand scans acquired using the structured light technology. According to [4] it is the first publicly available database where a hand was scanned using the structured light technology and both sides of a hand were captured within one scan. This paper presents hand recognition algorithm capable of processing 3D hand scans from the *DMCSv1* database.

The paper is organized as follows: Section II contains state of the art review. Section III describes the process of segmentation, feature extraction and classification proposed by the authors. Section IV presents the results obtained for the *DMCSv1* database. Finally, Section V presents the conclusions and future plan.

The project was funded by the National Science Centre on the basis of the decision number DEC-2011/01/D/ST6/06269.

P.S. Nowak, W. Sankowski, P. Krotewicz and M. Zubert are with the Department of Microelectronics and Computer Science, Lodz University of Technology (address: Wólczańska 221/223, 90-924 Łódź, Poland; e-mail: {psn, wsan, pkrotewicz, mariuszz}@dmcs.p.lodz.pl).

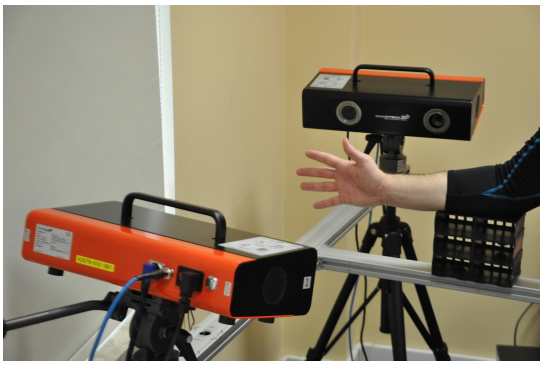

Fig. 1. 3D data acquisition station (hand scannig process).

II. State of the Art

Hand identification systems described in the literature can be classified into the following categories (see Fig. 2):

- Contact based
  - Pose invariant - devices with pegs or other guiding parts, user is obliged to place hand matching predefined pattern,
  - Pose variant - devices without any hand pose guidance, user is obliged to put hand on a flat surface.
- Contact free
  - Systems without any surface or form of guidance like pegs. Such systems are regarded as more user friendly and more natural [5].

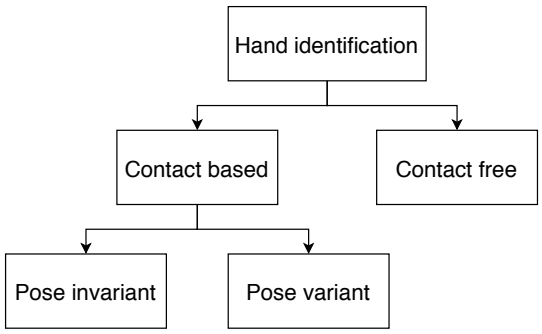

Fig. 2. Hand identification systems classification.

Hand identification systems could be also classified into one of three groups depending on implemented approach of geometric features extraction:

- hand contour,
- hand geometry,
- palm print.

Depending on acquisition sensor there are two possible data types:

- two-dimensional,
- three-dimensional.

Majority of methods described in the literature is based on 2D contact based methods of hand data acquisition. Only the latest publications go beyond rooted in history contact based solutions and introduce 3D algorithms for contact free systems.

A. Hand Contour

Research which describes person identification using hand contour is described in [6]. The researchers propose two algorithms that use hand contour data for person identification. The first method applies Hidden Markov Model (HMM) as the hand contour data based classifier. The results for HMM classifier show success rate equal to 70% tested on the main database subset that contains samples from 60 users. The second method for person identification uses Hidden Markov Model Kernel (HMMK) for hand contour features description and supervised Support Vector Machine (SVM) as a classifier. Success rate increased with the second method and reached 100%. The HMMK with SVM method was, as previously mentioned, tested on a subset that contains samples from 60 users from the main database collected for the research (see Table I).

TABLE I
CHARACTERISTICS OF DATABASE USED IN [6]

Number of classes	144
Number of samples per class	10
Acquisition and quantification	Gray scale (8 bits, 256 levels)
Resolution	150 dpi
Size	1403 x 1021 pixels

B. Hand Geometry

These methods are commonly used. They appear in studies of 2D as well as 3D data processing. They have been used since 1997. Origins of these methods go back to 1970's.

Methods developed for person classification based on hand geometry features are described in [7]. The described methods were evaluated using University of Nevada at Reno (UNR) and the University of Notre Dame (UND) datasets. Researchers presented in [7] the geometric-based method where extraction of 31 hand features was proposed for identification. Next the component-based approach using Zernike Moments is presented in [7]. This method segments hand into regions containing fingers or palm print. It is expected that splitting hand components will bring higher success rate for person identification in comparison to single geometrical descriptor of a hand. Each component is analysed separately and finally collective result is calculated for person recognition. The third method presented in [7] employs finger surface analysis, where certain fingers are considered: index, middle and ring finger. In this method additional normalisation is applied. Segmented finger is rotated and centred for further calculation. The extracted feature is the curvature of each of listed fingers.

According to [7] Zernike methods come with high computational cost compared to other proposed methods. On the other hand component based approach is limited due to registered image details and overall amount of details available for hand feature extraction. Zernike descriptor doesn't have limitation in this case. Table II contains results of described methods, where EER is Equal Error Rate, TAR is True Acceptance Rate and FAR is False Acceptance Rate.

TABLE II
TEST RESULTS REPORTED IN [7] FOR UND DATABASE

Method	Geometric	Zernike moments	Finger surface
EER [%]	10.2	1.72	5.5
TAR (FAR = 5%)	76.7	99.3	94.0

C. Palm Print

A method based on palm print surface processing is 3D equivalent of 2D contour methods. It can be classified as pose invariant identification. A research in this area is presented in [2], [8] and [9]. The papers mention about an important disadvantage of existing systems. They describe the impact of hand pose during hand based person identification. Papers [8] and [9] refer to [5], [10], [11], [12] for unconstrained pose hand identification. Researchers in [8] and [9] formed a hypothesis that it is necessary to standardize pose of acquired image data to build an effective identification system. In the process of normalisation, the algorithm finds centre of the palm and corrects pose of the hand using the normal vector of the hand surface. Table III describes effectiveness of these methods. The proposed algorithms were evaluated on a database collected for the research that contains samples from 177 individuals, 10 images per person acquired in two sessions.

TABLE III
TEST RESULTS REPORTED IN [8] AND [9]

Method	EER [%]	
	Without pose Correction	With pose Correction
2D Palm Print	11.80	1.1
3D Palm Print	16.32	1.61
2D Hand Geometry	28.69	21.15
3D Hand Geometry	40.9	17.2

D. Pose Correction

The system presented in [2], [8] and [9] was designed based on combined 2D and 3D image processing. There are 5 processing paths in the algorithm for each extraction type:

- 2D Finger processing with Gabor Filter,
- 2D Palm print processing with Gabor Filter,
- 2D Hand Geometry Features processing,
- 3D Finger Features processing,
- 3D Palm print Surface processing.

A person recognition system based on hand geometry presented in [2], [8] and [9] uses geometry features like: finger width, length etc., which are calculated based on finger tip and valley location. 3D finger surface and palm print segmentation is considered a new approach. Results presented in Table IV show that improvement in hand identification can be achieved with combined processing of 2D and 3D data. Method described in [2], [8] and [9] has its limitations, it is sensitive to fingers bending and to large hand plane rotation.

E. Synopsis

Researches referenced in this paper prove that at current state of biometrics evolution, improved results can be achieved with a fusion of different methods. Next finding is that hand pose normalisation significantly increases effectiveness of identification process as shown in [2], [8] and [9]. Zernike Moments solution is close to results in Table IV representing hand geometry research in [2], [8] and [9]. Results from contact free research [2], [8] listed in Table IV show that combined methods give better accuracy in comparison to other approaches presented in this paper.

TABLE IV
HAND RECOGNITION EVALUATION BASED ON [2]

Method	EER [%]
3D Hand Geometry	3.5
2D Hand Geometry	6.3
(2D+3D) Hand Geometry	2.3
2D Palm Print	1.22
3D Palm Print	3.16
(2D+3D) Palm Print	0.56
Finger Texture	6
Finger Texture + 2D Hand Geometry + 2D Palm Print	0.55
Finger Texture + (2D+3D) Hand Geometry + (2D+3D) Palm Print	0.22

III. THE ALGORITHM

General scheme of the algorithm for biometric person identification based on 3D hand scans proposed by the authors is presented in Fig. 3. The algorithm consists of three main stages:

- segmentation,
- feature extraction,
- comparison.

Initially, the algorithm processes a hand scan and returns a set of feature points for segmented parts of the hand. Next, features are extracted from the results of the segmentation phase and returned as a vector of features. The feature vector is compared with feature vectors saved in the database, in each comparison a score in the range $\langle 0, 1\rangle$ is calculated. The score

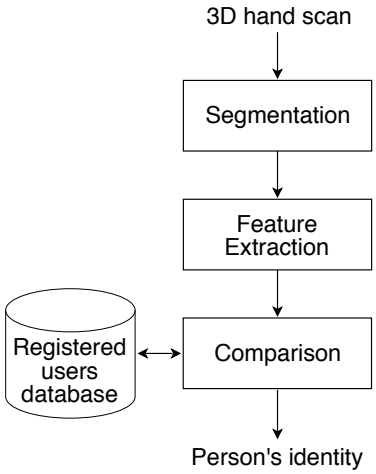

Fig. 3. Hand identification algorithm.

indicates dissimilarity between compared scans. Finally the comparison algorithm determines person's identity based on the lowest dissimilarity score obtained.

The presented research uses hand scans from the *DMCSv1* database [4]. Sample 3D hand scan from the database is depicted in Fig. 4. The hand scan is a set of (x, y, z) points organized in a point cloud data structure given by (1), where N is the number of points. The approach presented by the authors does not use colour information included in the scans.

$$A = \{(x_i, y_i, z_i);\ i = 0, ..., N-1\},\ A \subset R^3 \qquad (1)$$

Fig. 4. Sample 3D hand scan from the *DMCSv1* database.

A. Segmentation

The segmentation algorithm is divided into five steps (see Fig. 5):

- normalisation,
- projection,
- 2D preprocessing,
- 2D coarse segmentation,
- 2D precise segmentation.

The normalisation locates three characteristic points (see Fig. 6):

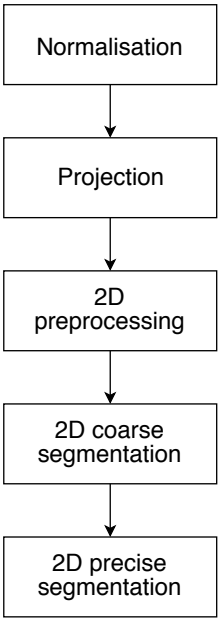

Fig. 5. Segmentation algorithm.

- middle finger tip denoted by O,
- centre of gravity of forearm denoted by F,
- thumb finger tip denoted by T.

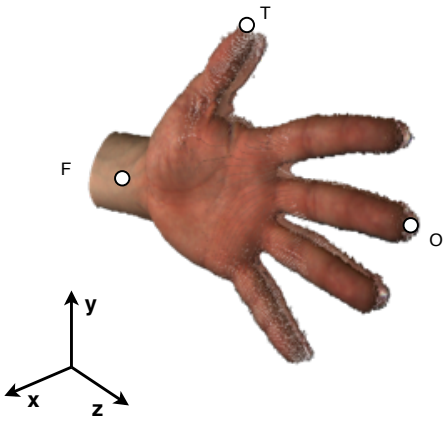

Fig. 6. Hand scan characteristic points.

The purpose of normalisation is to unify hand scan orientation for further processing. The normalised subset of hand scan point cloud A is denoted by A'. First of all, the middle tip point O (see Fig. 6) is found. It's a point in the point cloud that has maximal value of z coordinate, it's defined with (2). Points which are further from the middle finger tip point O than the defined hand scan length are removed from the processed scan. This length is experimentally set to 240 mm. Next, the point F is reconstructed by computing the coordinates (x_F, y_F, z_F) of the centre of gravity in the segment of the forearm point cloud. The segment is defined by a fixed number of points that are located around OZ axis closest to the border of the forearm. Equation for x coordinate of the F point is presented in (3), where x_i denotes the x coordinate of the i-th point and M is the number of points in the forearm segment. Coordinates y_F and z_F are calculated similarly. The thumb finger tip T (see Fig. 6) is found as a point in the point cloud that is characterised by maximal y coordinate, as given by (4).

$$z_O = \underset{(x_i,y_i,z_i)\in A}{max\, z_i} \tag{2}$$

$$x_F = \frac{1}{M}\sum_{i=0}^{M-1} x_i \tag{3}$$

$$y_T = \underset{(x_i,y_i,z_i)\in A}{max\, y_i} \tag{4}$$

Next, the points F, T, O are used to calculate vectors $\vec{V_{OX}}$ and $\vec{V_{OY}}$ presented in Fig. 7. Calculations are performed using (5) and (6).

$$\vec{V_{OX}} = \vec{V_{OT}} \times \vec{V_{OF}} \tag{5}$$

$$\vec{V_{OY}} = \vec{V_{OF}} \times \vec{V_{OX}} \tag{6}$$

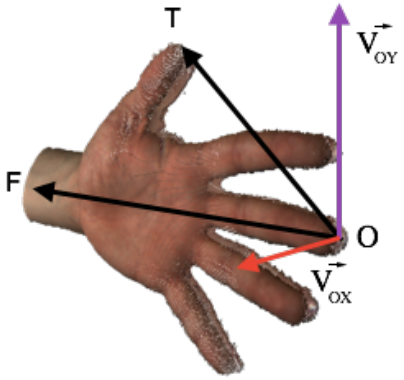

Fig. 7. Normalised coordinate system.

Finally a transformation to a new coordinate system is calculated, where obtained vectors define axes as follows: $\vec{V_{OF}}$ sets OZ axis, $\vec{V_{OX}}$ sets OX axis and $\vec{V_{OY}}$ sets OY axis of the new coordinate system. The middle finger tip point O is set as the origin point of the new coordinate system.

Normalised hand scan is transformed to a 2D image using the projection to YZ plane. Result of the projection is presented in Fig. 8.

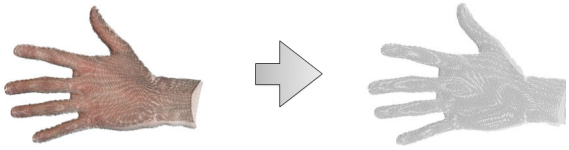

Fig. 8. Left - 3D hand scan, right - hand scan projection.

The projected image contains holes which have to be filled in. To fill those holes morphological operations - closing and opening - are applied to projected image. Both morphological operations use kernel of circular shape. Result is presented in Fig. 9. Then the shape analysis process starts. The algorithm searches the hand shape border points and returns a hand

contour. Presented algorithm uses the method described in [13] for contour finding.

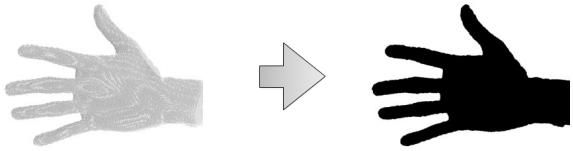

Fig. 9. Hand image before morphological operations - left, after morphological operations - right.

The set of feature points is defined as a vector containing 5 tip points and 6 valley points presented in Fig. 10. Initially, the feature points are found coarsely, next the coarse feature points location is refined. Coarse hand segmentation starts with reference point calculation as presented in Fig. 11. The reference point is located in the middle point of the forearm and for each contour point the euclidean distance to the reference point is calculated as shown in Fig. 12. The distances calculated for sample hand scan are presented in Fig. 13, those values are used to localize the tip and valley points. The tip point of each finger is the point in finger contour with large distance to the reference point. The valley point is the contour point between two fingers which distance from the reference point is the smallest.

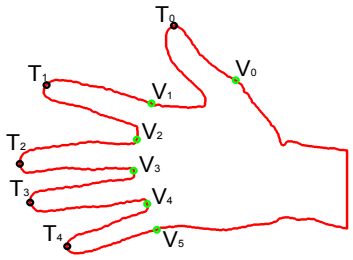

Fig. 10. Hand contour with tip and valley points.

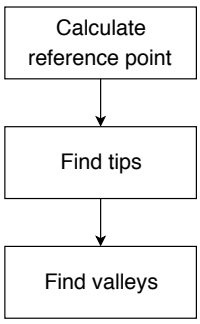

Fig. 11. 2D coarse segmentation.

For each contour point a derivative is calculated using distance values, result is presented in Fig. 14. To localize tip points of the fingers a kernel based matching is applied to the calculated derivative values. The matching algorithm computes correlation between kernel pattern presented in Fig. 15 and distance values presented in Fig. 14 and returns fitness measure presented in Fig. 17. The maximal values of the fitness measure match tip points. Each finger is defined by

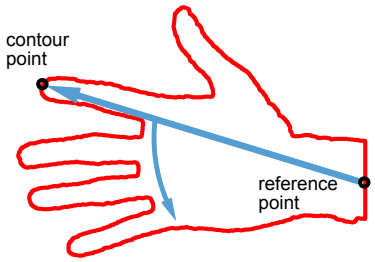

Fig. 12. Distance computed in 2D coarse segmentation.

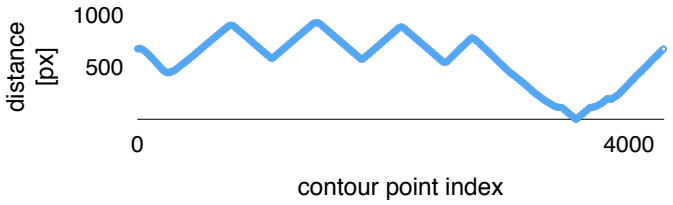

Fig. 13. Distances between contour points and reference point.

three points, a tip point and two neighbouring valley points. Valley points are calculated using tip points position.

First, the points V_2, V_3, V_4 (see Fig. 10) position is calculated. The method implemented for tip points localization is applied for the valley points localization also. The valley points search is performed using results from tip points localization which limits the contour to sections between tip points. The algorithm uses distance values between contour points and reference point (see Fig. 12). Valley point search is repeated for each pair of neighbouring fingers tips, it searches valley points between fingers: index and middle, middle and ring, ring and little. The valley points location is determined with kernel matching using kernel depicted in Fig. 16 that is applied to the derivative values presented in Fig. 14. Result for kernel matching is presented in Fig. 18. The contour points that correspond to the maximal values of the fitness measure are set as the valley points.

Then the valley points V_1 and V_5 (see Fig. 10) that belong to the index and little finger respectively are calculated based on the points V_2 and V_4. First the Euclidean distance between known valley point and tip point is calculated for each of these two fingers. The distance is used as a radius of a circle with centre in the finger tip. The circle has two important points of intersection with the contour, one is the known valley point, the second is the one that is being searched. Then using the same approach the point V_0 is calculated using the point V_1 position.

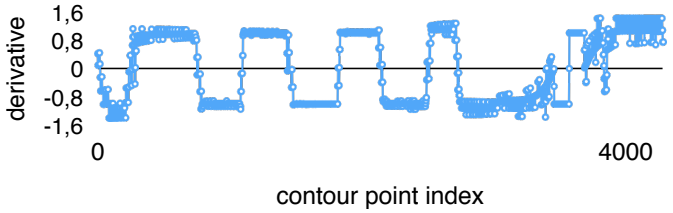

Fig. 14. Contour distances derivative.

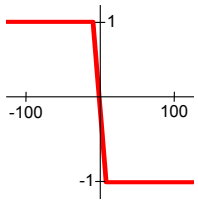

Fig. 15. Kernel for correlation function (tip points).

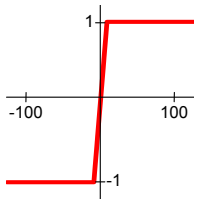

Fig. 16. Kernel for correlation function (valley points).

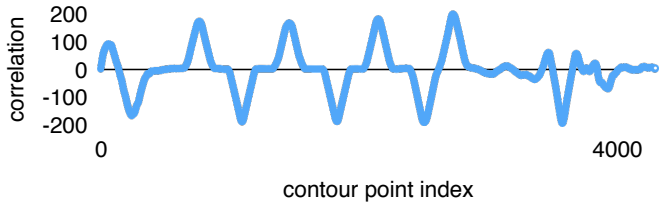

Fig. 17. Correlation result (tip points).

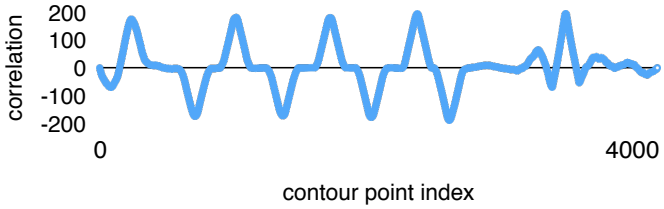

Fig. 18. Correlation result (valley points).

Next the precise segmentation module executes the coarse segmentation algorithm for each finger contour. The global reference point is replaced with a local one calculated for each of processed fingers as presented in Fig. 19. The local reference point is computed as the middle point between valley points that were found in the coarse segmentation. The precise algorithm is repeated iteratively. Number of iterations is experimentally set to 10. Finally, refined tip and valley points are returned. Result containing 5 tip points and 6 valley points found in the segmentation is presented in Fig. 20.

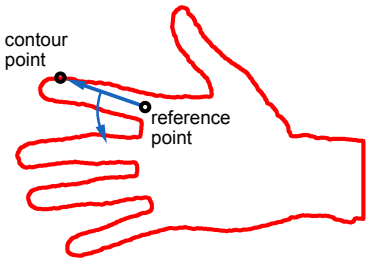

Fig. 19. Distance computed in 2D precise segmentation.

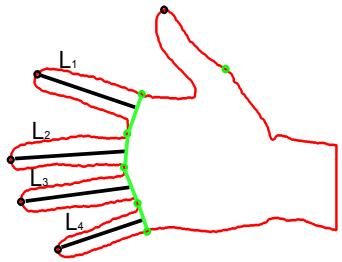

Fig. 20. Identification features (finger lengths).

B. Feature Extraction and Comparison

Tip and valley points are used to calculate features for identification. Presented algorithm uses length of four fingers for identification purposes. Experiments have shown that the thumb features are less distinctive than features of other fingers, therefore features of the thumb finger are excluded from further processing. Extracted feature vector F is given by (7), where $L_1, L_2, ..., L_4$ are lengths of fingers as shown in Fig. 20.

$$F = [L_1, L_2, L_3, L_4] \tag{7}$$

Comparison is performed for two feature vectors F_a and F_b, where a and b denote indices of the compared samples. Hand scans dissimilarity measure is calculated as in (8), where L_{ai} and L_{bi} denote length of the i-th finger in sample a and b respectively and S is the feature vector size which equals 4.

$$score = 1 - \frac{1}{S}\sum_{i=1}^{S}\frac{\min(L_{ai}, L_{bi})}{\max(L_{ai}, L_{bi})} \tag{8}$$

IV. Results

The algorithm presented in this paper was tested using the *DMCSv1* database [4]. The database is publicly available and contains samples acquired from 35 individuals in two sessions, 10 scans of left and 10 scans of right hand per individual per session (see Table V). The algorithm was tested on two subsets of *DMCSv1* database:

- left hand scans,
- right hand scans.

TABLE V
DMCSv1 DATABASE HAND SUBSET SPECIFICATION

Number of individuals	35
Number of sessions	2
Number of hand scans per individual per session	10 left hand 10 right hand
Total number of hand scans	35 x 2 x 20 = 1400
Files format	.ply (binary)

There is a set of samples for which the segmentation algorithm fails. Those samples are placed on the list of ignored samples. The set of ignored hand scans is automatically determined in the segmentation process when the algorithm detects insufficient number of tip or valley points in the hand scan. In the presented research 32 samples listed in Table

VI were rejected, where ID is the identification number of the individual in the database and Sample ID is number of sample of the individual. If for left or right hand the sample is segmented incorrectly then the sample with corresponding ID and Sample ID from the other hand is also ignored to maintain equal number of samples for both hands. Sample hand scan which is segmented incorrectly is depicted in Fig. 21. In this case hand rotation or incorrect finger pose causes that the expected location of a valley point V_3 is not obtained. Other samples that are rejected by the segmentation algorithm are depicted in Fig. 22 and Fig. 23.

TABLE VI
SAMPLES REJECTED IN THE SEGMENTATION

ID	Sample ID
4	5, 7, 8, 9, 18, 19, 20
5	11
8	20
20	1, 7, 9, 10
21	16
31	17
35	13

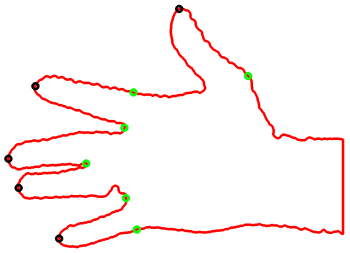

Fig. 21. Sample improper segmentation result (wrong location of point V_3).

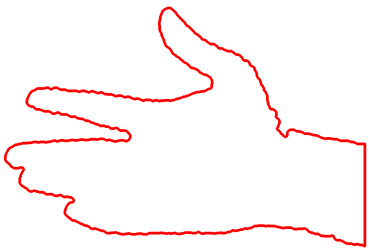

Fig. 22. Sample improper segmentation result (missing valley points).

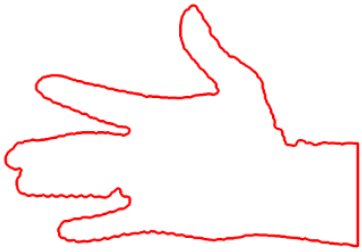

Fig. 23. Sample improper segmentation result (missing valley points).

Further evaluation of the algorithm was performed on the set of correctly segmented hand scans, which contains 1368 samples from total number of 1400 in the *DMCSv1* database [4]. The obtained values of Equal Error Rate (EER), Area Under Curve (AUC) and Rank-1 accuracy are presented in Table VII. Measurement uncertainty of EER presented in Table VII is determined for the 90% confidence level.

TABLE VII
RESULTS OBTAINED FOR THE *DMCSv1* DATABASE

	EER [%]	AUC	Rank-1 accuracy [%]
Left hand scans	16 ± 4	0.91	85
Right hand scans	17 ± 5	0.89	82

The Detection Error Tradeoff (DET) curves obtained for left and right hand scans are depicted in Fig. 24, where FRR is False Rejection Rate and FAR is False Acceptance Rate. The obtained Cumulative Match Characteristic (CMC) curves are presented in Fig. 25, where CRR is Correct Recognition Rate.

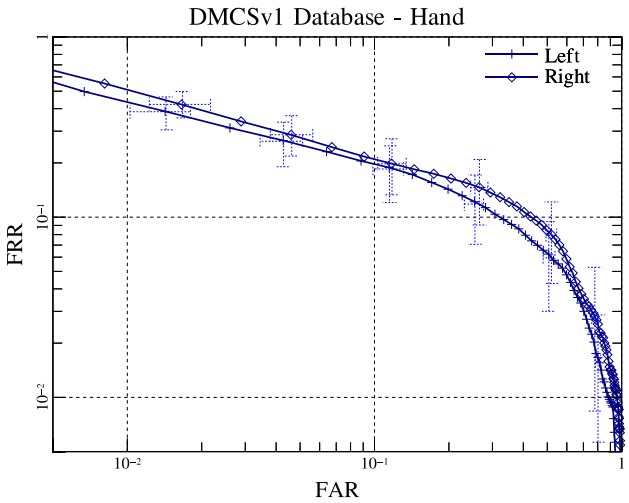

Fig. 24. DET curves obtained for the *DMCSv1* database.

V. CONCLUSIONS

In the paper the novel algorithm for person identification based on double-sided 3D scan of hand geometry proposed by the authors is presented. The algorithm was evaluated on the publicly available *DMCSv1* database. Obtained values of equal error rate are 16% for the left hand scans, 17% for the right hand scans and the values of rank-1 accuracy are 85% and 82% for the left and right hand scans, respectively. The results show that hand geometry features are unique for an individual, but cannot be used solely for persons identification. Due to high error rates they are rather appropriate for use in multimodal than unimodal biometric systems.

The aims for the future comprise improving segmentation algorithm and adding more features in the feature extraction phase. The authors also plan to fuse results obtained from left and right hand scans.

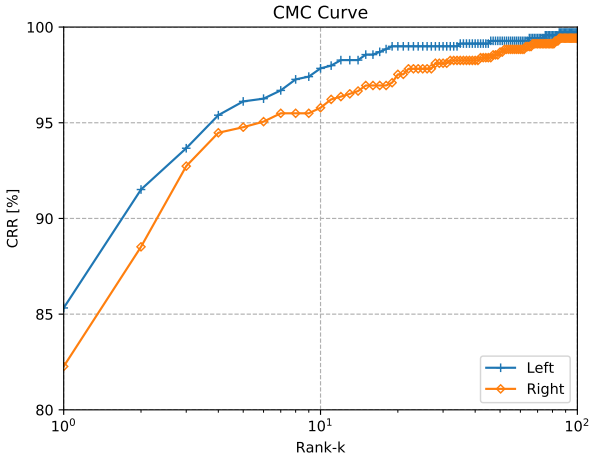

Fig. 25. CMC curves obtained for the *DMCSv1* database.

REFERENCES

[1] A. Ross, "An introduction to multibiometrics," in *2007 15th European Signal Processing Conference*, Sept 2007, pp. 20–24.

[2] V. Kanhangad, A. Kumar, and D. Zhang, "A unified framework for contactless hand verification," *IEEE Transactions on Information Forensics and Security*, vol. 6, no. 3, pp. 1014–1027, Sept 2011.

[3] Department of Microelectronics and Computer Science, "Multimodal biometric system for contactless persons identification," 2015. [Online]. Available: http://www.biometrics.dmcs.pl/en/projects/mbs

[4] W. Sankowski, P. S. Nowak, and P. Krotewicz, "Multimodal biometric database dmcsv1 of 3d face and hand scans," in *Mixed Design of Integrated Circuits Systems (MIXDES), 2015 22nd International Conference*, June 2015, pp. 93–97.

[5] V. Kanhangad, A. Kumar, and D. Zhang, "Combining 2d and 3d hand geometry features for biometric verification," in *2009 IEEE Computer Society Conference on Computer Vision and Pattern Recognition Workshops*, June 2009, pp. 39–44.

[6] J. C. Briceno, C. M. Travieso, J. B. Alonso, and M. A. Ferrer, "Biometric identification based on hand-shape features using a hmm kernel," in *Hand-Based Biometrics (ICHB), 2011 International Conference on*, Nov 2011, pp. 1–6.

[7] G. Amayeh, G. Bebis, and M. Hussain, "A comparative study of hand recognition systems," in *Emerging Techniques and Challenges for Hand-Based Biometrics (ETCHB), 2010 International Workshop on*, Aug 2010, pp. 1–6.

[8] V. Kanhangad, A. Kumar, and D. Zhang, "Contactless and pose invariant biometric identification using hand surface," *IEEE Transactions on Image Processing*, vol. 20, no. 5, pp. 1415–1424, May 2011.

[9] V. Kanhangad, A. Kumar, and D. Zhang, "Human hand identification with 3d hand pose variations," in *2010 IEEE Computer Society Conference on Computer Vision and Pattern Recognition - Workshops*, June 2010, pp. 17–21.

[10] S. Malassiotis, N. Aifanti, and M. G. Strintzis, "Personal authentication using 3-d finger geometry," *IEEE Transactions on Information Forensics and Security*, vol. 1, no. 1, pp. 12–21, March 2006.

[11] A. Kumar, "Incorporating cohort information for reliable palmprint authentication," in *Computer Vision, Graphics Image Processing, 2008. ICVGIP '08. Sixth Indian Conference on*, Dec 2008, pp. 583–590.

[12] A. Morales, M. A. Ferrer, F. Díaz, J. B. Alonso, and C. M. Travieso, "Contact-free hand biometric system for real environments," in *Signal Processing Conference, 2008 16th European*, Aug 2008, pp. 1–5.

[13] S. Suzuki and K. Abe, "Topological structural analysis of digitized binary images by border following," *Computer Vision, Graphics, and Image Processing*, vol. 30, pp. 32–46, 1985.

Piotr Stefan Nowak received the MSc degree in Computer Science from Lodz University of Technology in 2012. He started PhD studies and currently is the PhD candidate in Computer Science. His interests include 2D and 3D image processing including applications in biometrics, architectures of distributed systems and internet of things.

Wojciech Sankowski received the MSc degree in Electronics and Telecommunication from Lodz University of Technology in 2004. In 2009 he received the PhD degree in Computer Science from the same university. From 2009 till 2011 he worked in the software industry as a senior software developer in TomTom Content Production Unit. Since 2011 he works as an assistant professor at Lodz University of Technology. His research interests include image processing algorithms dedicated for biometrics and fusion of multiple biometric traits.

Paweł Krotewicz received the MSc degree in Computer Science and Information Technology from Lodz University of Technology in 2014. He started PhD studies and currently is the PhD candidate in Computer Science. Meanwhile he worked in the software industry as a C++ Senior Software Developer in Mobica Limited and Tieto companies. His field of expertise comprises new standards of C++ programming language, image processing algorithms for biometrics and machine learning.

Mariusz Zubert received the MSc and PhD degrees in Electronics from Lodz University of Technology in 1995 and 1999 respectively. He received the DSc degree in Computer Science in December 2010. His interests include modelling, simulation and reduction of systems with a special consideration of the distributed multidomain phenomena and power-cable state and rating estimations, heat transfer as well as expert systems based on image processing, statistical methods and 3-D image reconstruction used for medical diagnosis of neurodegenerative diseases.